GLOBAL JOURNAL OF ENGINEERING RESEARCH VOL. 4 NO. 1&2, 2005: 31 - 38
 ISSN 1596-292X

A RECEDING EVAPORATIVE FRONT MODEL FOR THE DRYING CHARACTERISTICS OF A FLAT PLATE 1: THEORY

Y. T. PUYATE

(Received 5 January 2004; Revision accepted 2005)

ABSTRACT

A theoretical background study is presented for the pressure and moisture distributions, stress and strain produced during the drying process of an elastic flat plate with a receding evaporative front. A three-stage drying process is proposed. In the first stage (saturated stage), the body is fully saturated and pressure-driven flow prevails. During the second stage (partially saturated stage), the evaporative front recedes through the material and divides the material into saturated and unsaturated zones. During the third stage (fully unsaturated stage), the body is entirely unsaturated and moisture is lost by diffusion only. An exact model for the falling-rate period of drying of solids, during which a body may be partially saturated or fully unsaturated, is also presented based on Sherwood's diffusion theory. The exact model is compared with Sherwood's approximate models for the falling-rate period, and with experimental data. The agreement between the exact model and the experimental data is shown to be better than that between the experimental data and Sherwood's models for the given drying rate.

KEYWORDS: Drying; Flat plate; Solid; Receding; Evaporative front.

INTRODUCTION

There is the need to characterize properly the drying behaviour of a flat plate, considering the growing trend and horizon of chemical processes involving film formation. At small moisture levels, a wet material is brittle, and deforms in an elastic manner under load (Keey, 1975). Such a material will return to its original condition on drying. More generally, a moist material exhibits both elastic and plastic behaviuor. An ideal elastic-plastic solid deforms linearly with load to the elastic limit. Further deformation beyond the yield point induces plastic flow, and the solid deforms continuously with no increase in stress.

The principles of flow in porous media are of such general interest that they have been frequently "rediscovered", and relevant literature is found in fields including wood technology, biotechnology, soil science, food science, membrane science, concrete structures, and polymer science, as well as ceramics. In most cases, liquid flows through a porous body in response to a gradient in pressure; at the same time, the pressure can cause deformation of the solid network and dilation (or shrinkage) of the pores through which the liquid flows.

Scherer (1987a, 1987b, 1990) showed how to develop a capillary flow model for drying of porous bodies in which loss of moisture is accommodated by shrinkage of the body, and elastic stress is developed to balance the capillary tension in the pore liquid. Darcy's Law was applied to derive a diffusion equation for the pressure distribution within the porous body, and solved using a two-stage model for drying. In the first stage of the model (the constant-rate period), the evaporation rate is constant and the capillary tension within the body rises. A critical point is reached when the capillary tension reaches a maximum value at the free surface, and this marks the end of the first stage. In the second stage of the model (the falling-rate period), the capillary tension at the free surface remains fixed at the maximum value and the drying rate gradually decreases. In this approach, the drying front is effectively pinned at the free surface, which is inconsistent with reality.

Earlier models for drying, following from the work of Sherwood (Sherwood, 1931; Gilliland and Sherwood, 1933), were based on mass transfer of moisture by diffusion within the porous medium. In these models, no account is taken of the capillary tension or of the stress and strain developed within the porous body. There is a constant-rate period in which the evaporation rate of liquid is constant and the moisture content of the body falls. The moisture content at the free surface falls to its equilibrium value at the end of the constant-rate period, and remains constant during the falling rate period that follows immediately.

Scherer's (1987a, 1987b, 1990) and Sherwood's (Sherwood, 1931; Gilliland and Sherwood, 1933) models for drying are both quite widely used, yet are based on quite different paradigms. The Scherer model is based on capillary flow, and is clearly appropriate for the initial stage of drying when the body is saturated. The Sherwood model is based on moisture diffusion through the porous body and is clearly appropriate when the body is nearly dry, the pores are filled mostly with air, and the liquid exists in isolated pendular drops. Neither model is entirely satisfactory, though both have been used, for intermediate stages of drying when the pores are largely filled with air but the liquid exist in a funicular state forming a continuous connected network in the body.

As proposed in the current study, the drying process of a body may be divided into three distinct stages (see Fig. 1, which shows a film of drying material in a container). In the first stage, the body is fully saturated, there is continuous liquid flow path to the surface, and capillary flow prevails. The adjacent film of air is maintained in a saturated state (with respect to moisture vapour) so that the surface behaves as free surface and the evaporation rate is constant. During the second stage, a liquid-gas interface (i.e. the evaporative front) recedes through the material and divides it into two regions; the interior of the material remains saturated up to the interface, while the exterior part of the material is unsaturated but has some residual liquid contained in isolated pendular drops. The second stage ends when the interface reaches the centre of a body that is dried from both sides, or the unexposed face of a body that is dried from only one side, and the saturated region is obliterated. During the third stage, which may be relatively short, the body is entirely unsaturated and moisture is lost by diffusion only. The three stages are thus termed the *saturated stage*, the *partially saturated stage*, and the *fully unsaturated stage*. Note that in Fig. 1, the critical point can occur in any of the three

Y. T. PUYATE, Dept. of Chemical Engineering, Rivers State University of Science and Technology, Port Harcourt, Port Harcourt, Nigeria

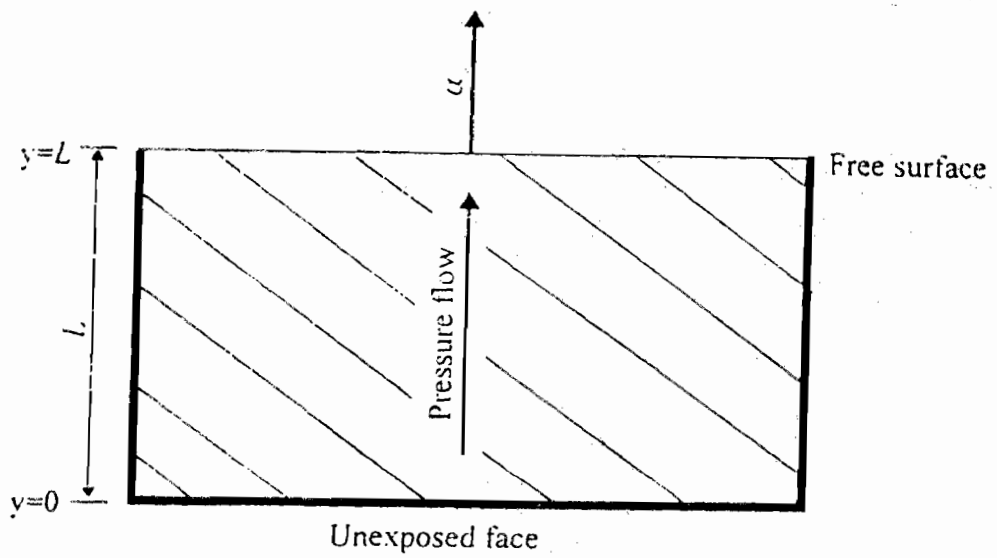

Fig. 1(a). Saturated stage

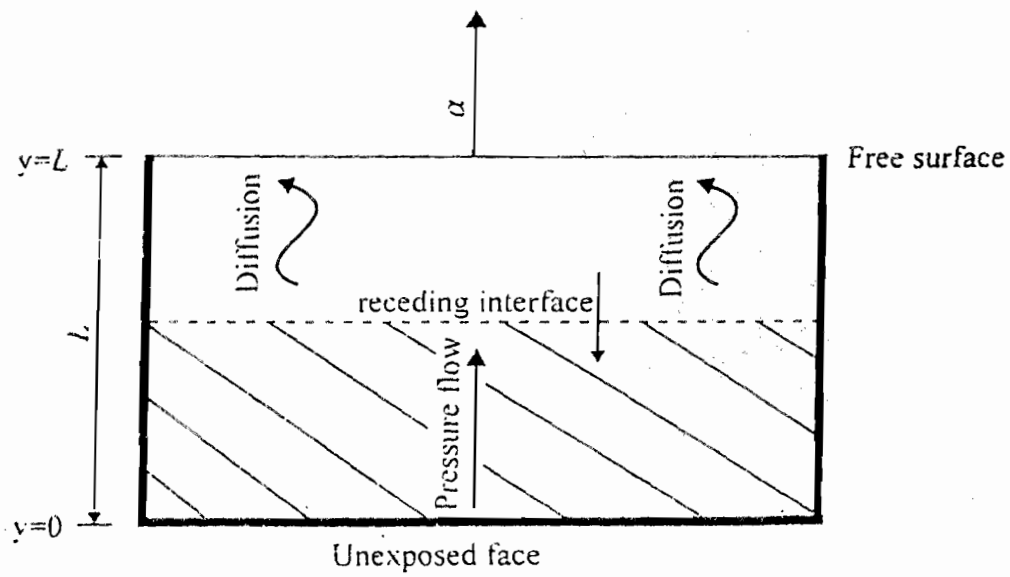

Fig. 1(b). Partially saturated stage.

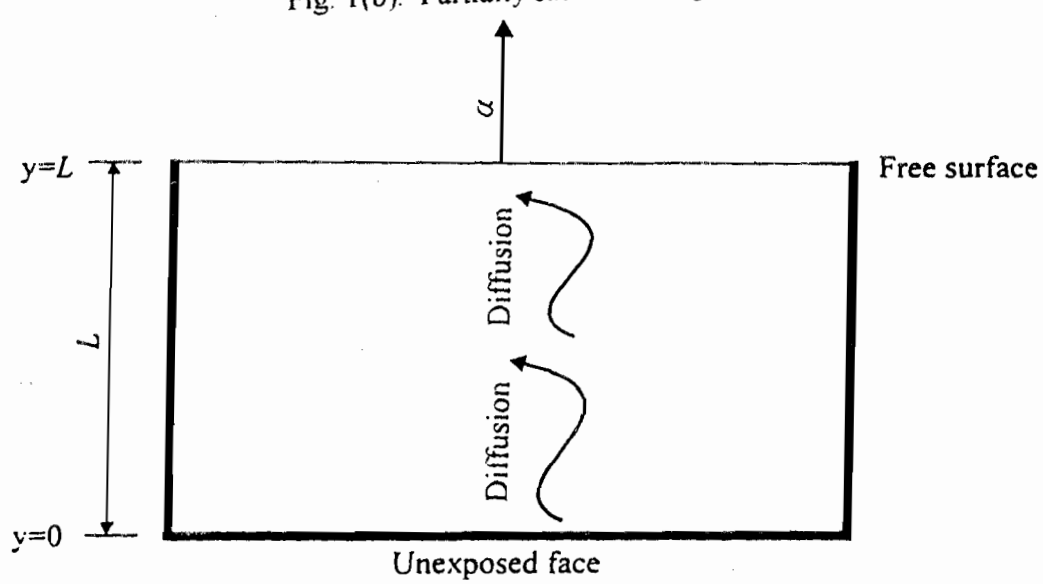

Fig. 1(c). Fully unsaturated stage

Fig. 1. Schematic diagram of the three stages of drying

stages depending on the drying conditions, where α is the rate of drying per unit area in the constant-rate period, and L is the thickness of the material. Most of the stress build-up and shrinkage occur during the saturated stage, although as shown in Part II of the series, some stress also occurs during the partially saturated stage.

This paper presents a theoretical background study for the pressure, moisture, stress and strain distributions, in a three-stage drying process of an elastic flat plate with a receding evaporative front. An exact model for the falling-rate period of drying of solids based on Sherwood's diffusion theory, which will be applied in Parts II and III of this series is also presented.

Capillary pressure

When liquid evaporates from a porous body, elements of both solid and liquid surfaces are exposed. For a wetting liquid (contact angle $\theta < \pi/2$), the energy (γ_{SV}) of the solid-vapour interface is greater than the energy (γ_{SL}) of the solid-liquid interface, and the liquid tends to flow to cover the exposed solid surface. As the liquid stretches towards the exterior, it goes into tension and this has two consequences: (i) liquid tends to flow from the interior down the pressure gradient, according to Darcy's Law, and (ii) the tension in the liquid is balanced by the compressive stress in the solid network that causes shrinkage (Scherer, 1990; Brinker and Scherer, 1990). Since the volume of liquid in the material is reduced by evaporation, the meniscus must become curved at the surface in such a way that the pressure within the liquid is lower than that in the surrounding air (a concave meniscus). The difference in pressure across a spherical meniscus is given by (Ford, 1986)

$$\Delta p = \frac{2\gamma_{LV}}{r} \qquad (1)$$

where γ_{LV} is the liquid-vapour interfacial energy (or surface tension), and r is the radius of curvature of the meniscus. If the surface is flat (that is, no meniscus curvature), then $r \to \infty$ and $\Delta p = 0$. The pressure difference Δp is the difference between the ambient atmospheric pressure (p_{atm}) and the pressure in the liquid (p_L), and is referred to as the capillary tension in the liquid (φ) ; that is, $\varphi = p_{atm} - p_L$. Thus $\varphi > 0$ as long as the liquid remains in tension. As liquid is evaporated from the surface of the drying material, the radii of curvature of surface menisci will decrease, thereby increasing the capillary tension according to eq. (1). The tension in the liquid gradually rises, and is supported by the solid phase, which therefore goes into compression. If the network is compliant, the compressive stress will cause it to contract into the liquid and the meniscus remains at the exterior surface. As drying proceeds, the network becomes increasingly stiff, because of the formation of new bonds and the decrease in porosity; the meniscus becomes more curved and the tension in the liquid rises correspondingly. Once the radius of the meniscus is small enough to enter the pores,, the liquid exerts the maximum possible tension. That marks the end of the saturated stage; beyond that point the tension in the liquid cannot overcome further stiffening of the network, so the meniscus recedes into the pore leaving air-filled pores and isolated pendular liquid drops near the surface. Thus during the saturated stage, the shrinkage of the body is equal to the volume of liquid evaporated; the meniscus remains at the exterior surface, but its radius r decreases continuously.

The end of the saturated stage is called the *entry point*, at which the radius of the meniscus is small enough to fit into the pores. The maximum capillary tension exerted by the liquid at the entry point is given approximately by (Scherer, 1990)

$$\varphi_{\max} = \gamma_{LV} \cos(\theta) S \rho_{bd} / \phi \qquad (2)$$

where S is the specific surface area of a porous body (area per unit mass of solid phase), ρ_{bd} is the *bulk density* of the solid network (not counting the mass of liquid; that is, the mass of the solid phase divided by the total volume), and ϕ is the porosity of the material. Thus $1-\phi$ is the solid volume fraction. According to previous theories (Scherer, 1987b, 1990; Brinker and Scherer, 1990), after $\varphi = \varphi_{\max}$ at the exterior surface, the evaporative front remains fixed at the surface, and the tension rises in the interior of the body until $\varphi = \varphi_{\max}$ in the liquid throughout the body. In these previous theories, the constant-rate period ended when $\varphi = \varphi_{\max}$ at the exterior surface, and this marked the beginning of the falling-rate period.

However, in the current study, when $\varphi = \varphi_{\max}$ at the exterior surface, the evaporative front is drawn into the material and the body is then only partially saturated. The equations for saturated flow prevail in the saturated region of the body, and the capillary tension at the interior evaporative front remains at $\varphi_{\max}$ as the evaporative front recedes into the body. Mass transfer in the unsaturated region is by diffusion and follows approximate models developed by Sherwood (1929, 1931), whose exact form is presented in section 5.

Fluid transport in a porous body

The transport equation will be written in terms of the gauge pressure $P = p - p_{atm}$. Fluid flow through porous media obeys Darcy's Law (Scherer, 1990), which states that the flux of liquid is proportional to the gradient of pressure in the liquid; that is

$$J = -\frac{\kappa}{\eta_L} \nabla P_L \qquad (3)$$

where J is the flux of liquid with dimensions of volume per unit area of the porous body (not the area occupied by the liquid) per unit time, P_L is the gauge pressure in the liquid (force per unit area of the liquid), η_L is the viscosity of the liquid, κ is the permeability of the body and has units of area, and ∇ is the gradient operator. The most popular model for the permeability, because of its simplicity and qualitative accuracy, is the Carman – Kozeny equation which gives an approximation for the permeability in terms of the skeletal density and specific surface area as (Scherer, 1990)

$$\kappa = \frac{\phi^3}{5\left((1-\phi)S\rho_{sd}\right)^2} \tag{4}$$

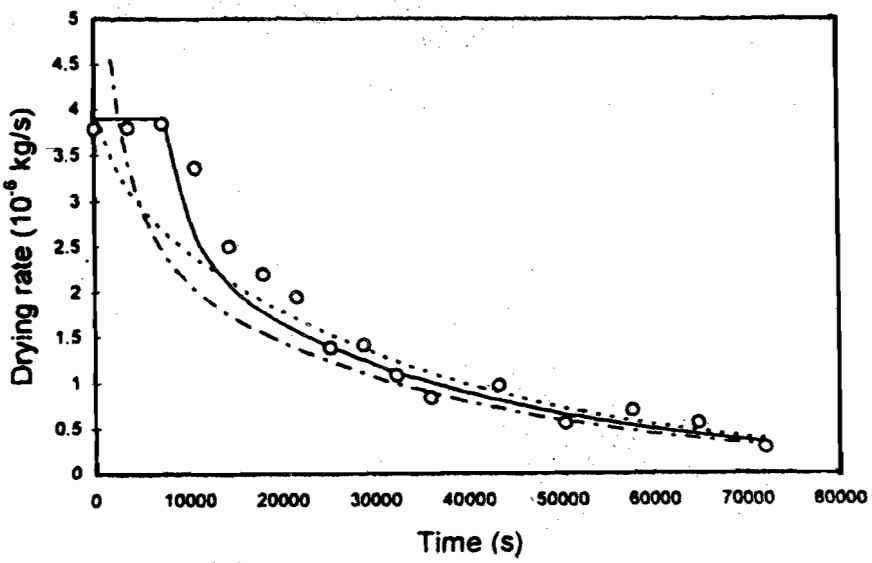

Fig. 2(a). Plot of drying rate against time.

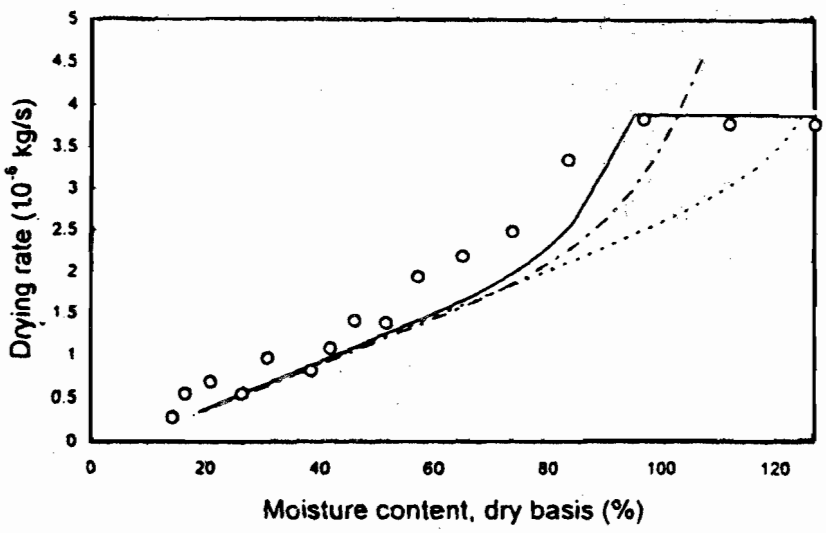

Fig. 2(b). Plot of drying rate against moisture content.

Fig. 2. Measured and predicted drying rate profiles for hemlock wood, $\mu = 2.94$.
o Measured values; _____ Exact solution (26); _____ Sherwood's high drying rate solution (27); _ _ _ _ _ _ Sherwood's low drying rate solution (28).

where ρ_{sd} is the *skeletal density* (the density of the solid skeleton; that is, the mass of the porous liquid-free network divided by the volume of the solid within the network). The factor 5 is an empirical correction for the non-circular cross-section and non-linear path of actual pores. This equation is reasonably successful for many types of granular materials, but it often fails and needs to be applied with caution.

If we consider an isolated region of a porous medium, the rate of change of the volume of liquid in that region depends on the divergence of the flux (that is, the difference between the flux leaving and the flux entering). During the saturated stage of drying when the pores are full of liquid, the change in the liquid content (using eq. (3)) must be equal to the change in pore volume,

which is equal to the volumetric strain rate, $\dot{\varepsilon}_{ll}$. Setting these changes equal, gives the equation for continuity (conservation of matter) in terms of the gauge pressure as

$$\dot{\varepsilon}_{ll} = -\nabla \cdot J = \frac{\kappa}{\eta_L} \frac{\partial^2 P_L}{\partial x_l^2} \tag{5}$$

where in index notation $i = 1, 2, 3$ and $x_1 = x$, $x_2 = y$, $x_3 = z$; the superscript dot indicates the partial derivative with respect to time, the repeated index (l) indicates summation, and κ and η_L are taken to be constant. Equation (5) applies during the saturated stage, and within the saturated zone of the partially saturated stage.

4. Stress in a saturated porous elastic body

In this section, the constitutive equation for a saturated porous elastic body is developed; that is, the relationship between the stress applied to the body and the strain that results. The stress (tensor) σ_{ij} acting on a saturated porous body is supported partly by the solid phase and partly by the liquid in the pores in the additive form

$$\sigma_{ij} = \sigma_{Lij} + \sigma_{Sij} \tag{6}$$

where σ_{Lij} is the stress (tensor) acting on the liquid phase, and σ_{Sij} is the stress (tensor) acting on the solid phase. (That is, the force on the respective phase per unit of the total surface area). If the matrix structure is isotropic, the stress in the liquid reduces to a pore pressure, which may be expressed in terms of the gauge pressure in the liquid as (Aris, 1962; Landau and Lifshitz, 1986)

$$\sigma_{Lij} = -\phi P_L \delta_{ij} \tag{7}$$

where ϕ is the pore volume fraction (void fraction), and δ_{ij} is the Kronecker delta. Note that we apply the gauge pressure convention also to the normal components of the stress so that the stress tensor is zero in an undeformed body. The stress carried by the solid matrix depends on the constitutive behaviour of the matrix in the absence of the liquid (that is, the hypothetical empty porous network when the liquid is drained away, not the dry body). Since both the solid and liquid phases are assumed to be incompressible, it is only the solid network that can comply to the capillary tension. If the network is assumed to be elastic, the stress supported by the solid matrix (or network) is given by (Landau and Lifshitz, 1986)

$$\sigma_{Mij} = \frac{E_p}{1+\nu_p}\left(\varepsilon_{ij} + \frac{\nu_p}{1-2\nu_p}\varepsilon_{ll}\delta_{ij}\right) \tag{8}$$

where E_p and ν_p are the Young's modulus and Poisson's ratio respectively for the porous matrix, σ_{Mij} is the force per unit of the total surface area, and ε_{ij} is the linear strain tensor given in terms of the displacement vector u_i by

$$\varepsilon_{ij} = \frac{1}{2}\left(\frac{\partial u_i}{\partial x_j} + \frac{\partial u_j}{\partial x_i}\right) \tag{9}$$

and assumed to be small. The stress σ_{Mij} is supported by the deformation of the matrix, and this stress exists only if the porous matrix is deformed. In an undeformed saturated porous material, the pressure in the solid phase must be equal to the pressure in the liquid. By analogy with eq. (7), the stress acting on the solid phase of an undeformed porous material is $-(1-\phi)P_L\delta_{ij}$. Addition of eq. (7) and the total stress borne by the solid phase, according to eq. (6), gives

$$\sigma_{ij} = -P_L\delta_{ij} + \frac{E_p}{1+\nu_p}\left(\varepsilon_{ij} + \frac{\nu_p}{1-2\nu_p}\varepsilon_{ll}\delta_{ij}\right) \tag{10}$$

Equation (10) is the constitutive equation for the stress acting within a saturated, porous, and isotropic elastic material. The objective is to determine the stress borne by the deformation of the matrix, which is

$$\sigma_{Mij} = \sigma_{ij} + P_L\delta_{ij} \tag{11}$$

In soil mechanics, this is termed the effective stress (Terzaghi et al., 1996). The equilibrium equation for quasi-static conditions, and for a case in which the deformation of a body is caused not by body forces but by forces applied to its surfaces (or in this case by pore pressure), may be obtained through Newton's Second Law of motion as

$$\nabla \cdot \sigma = 0 \text{ or } \frac{\partial \sigma_{ij}}{\partial x_i} = 0 \tag{12}$$

Using eq. (10) in eq. (12) gives a general form of the equilibrium equation for isotropic linear elastic saturated porous bodies as

$$-\frac{\partial P_L}{\partial x_j}+\frac{E_p}{1+\nu_p}\left(\frac{\partial}{\partial x_i}\varepsilon_{ii}+\frac{\nu_p}{1-2\nu_p}\frac{\partial}{\partial x_j}\varepsilon_{II}\right)=0 \qquad (13)$$

which upon operating through by $\partial/\partial x_j$ using eq. (9) gives

$$\nabla^2 P_L=\frac{E_p(1-\nu_p)}{(1+\nu_p)(1-2\nu_p)}\nabla^2\varepsilon_{II} \qquad (14)$$

Using eq. (14) in eq. (5) results in a diffusion equation for the volumetric strain ε_{II} in the form

$$\dot{\varepsilon}_{II}=D\nabla^2\varepsilon_{II} \qquad (15)$$

where $D=\kappa E_p(1-\nu_p)/\eta_L(1+\nu_p)(1-2\nu_p)$. An equation for P_L which is not a pure diffusion equation can be obtained by taking ∇^2 of eq. (5) through eq. (14) as

$$[(\partial/\partial t)-D\nabla^2]\nabla^2 P_L=0 \qquad (16)$$

In contrast to the current work, Scherer (1987b) made the additional assumption that for an elastic solid phase, the volumetric strain obeys the following constitutive equation (here written in terms of the gauge pressure)

$$\varepsilon_{II}=3\varepsilon_W+\frac{P_L}{K_p} \qquad (17)$$

where K_p is the bulk modulus of the porous matrix (not the modulus of the solid phase itself), and ε_W is said to be the linear strain caused by the solid-liquid interfacial energy, which is given by

$$\varepsilon_W=-\gamma_{SL}S\rho_{sd}(1-\nu_s)/E_s \qquad (18)$$

where ν_s and E_s are the Poisson's ratio and Young's modulus respectively for the solid phase. The strain ε_W was assumed to be present in a saturated body, and uniform throughout the body at the start of drying. By the implied assumption that ε_W is constant, the volumetric strain rate $\dot{\varepsilon}_{II}$ was obtained from eq. (17), and the resulting expression used in eq. (5) to give

$$\dot{P}_L=D_S\nabla^2 P_L \qquad (19)$$

where $D_S=K_p\kappa/\eta_L$. Equation (19) was then applied (Scherer, 1987b) to a flat plate that is dried from both sides. However, in view of the relationship (Landau and Lifshitz, 1986; Brinker and Scherer, 1990) $K_p=E_p/3(1-2\nu_p)$, the resulting value of D_S is slightly different from D above. For example, if ν_p is small (for highly compressible liquid-free network), then $D\approx 3D_S$ which indicates a significant difference between the two diffusion coefficients. Furthermore, the local equilibrium equation (10) was not used; therefore eq. (19) (unlike eq. (16)) is not consistent with the full system of equations (eqs. (5), (9), (10), and (12)). Equation (19) may, nevertheless, be a useful model equation. It will be seen in Parts II and III of this series that a diffusion equation for the pressure analogous to eq. (19), but with the diffusion coefficient D, may be rigorously derived for a flat plat with a fixed base. As in Scherer's model, both the drying stresses and strains are analysed in the current work through the pressure distribution.

5. Exact diffusion model for the falling-rate period

In any drying operation, the manner in which the water in the solid travels to the solid surface, and then out into the air, has an important influence on the rate of drying. According to the widely accepted Sherwood's theory in drying, all very wet solids being dried under constant drying conditions exhibit a period (called the *constant-rate period*) during which the rate of drying is constant. The rate, however, does not remain constant until the solid is dry, but at some intermediate moisture content called the *critical moisture content*, the rate starts to decrease and the range from the critical point to dryness is called the *falling-rate period*. The

equation proposed by Sherwood (1929) to govern mass transport inside all drying media is given by

$$\frac{\partial \rho}{\partial t} = D_m \frac{\partial^2 \rho}{\partial y^2} \tag{20}$$

where ρ is the moisture concentration (in mass units), D_m is the moisture diffusion coefficient, y is the distance of transport of moisture, and t is time. During the constant-rate period of drying a flat plate with a fixed base as in Fig. 1, the moisture gradient at the exposed face ($y = L$) is equal to the constant drying rate, while that at the unexposed face ($y = 0$) is zero at all time. With the assumption of a uniform moisture distribution at the start of drying, Gilliland and Sherwood (1933) presented a solution to eq. (20) based on the above conditions for the constant-rate period in dimensionless form as

$$\theta_1(Y,\tau) = 1 - \mu\left[\tau + \frac{Y^2}{2} - \frac{1}{6} - \frac{2}{\pi^2}\sum_{n=1}^{\infty}\frac{(-1)^n}{n^2}\exp(-n^2\pi^2\tau)\cos(n\pi Y)\right] \tag{21}$$

The dimensionless variables are defined as

$$\theta = \frac{\rho - \rho_{eq}}{\rho_o - \rho_{eq}} \qquad Y = \frac{y}{L} \qquad \tau = \frac{tD_m}{L^2} \tag{22}$$

where L is the thickness of the flat plate, ρ_o is the initial uniform moisture concentration, ρ_{eq} is the equilibrium moisture concentration, $\mu = \alpha L/(\rho_o - \rho_{eq})D_m$ is the drying intensity which relates the characteristics times for evaporation and liquid diffusion, and α is the rate of drying per unit area in the constant-rate period. When μ is large, evaporation is fast, large concentration gradients occur, and the constant-rate period is short. Conversely, when μ is small, evaporation is slow, the concentration gradients are small, and the constant-rate period is long. The total quantity of moisture, Θ, in the body at any time during the constant-rate period is obtained by integrating eq. (21) across the thickness to obtain

$$\Theta_1(\tau) = 1 - \mu\tau \tag{23}$$

Equation (20) still holds in the falling-rate period since the process is controlled by diffusion of free moisture. The initial condition of the falling-rate period corresponds to the moisture distribution at the end of the constant-rate period, which is given by eq. (21) at $\tau = \tau_{cr}$, where τ_{cr} is the dimensionless critical time. The moisture concentration at the surface of the body during the falling-rate period is the equilibrium moisture content, while the moisture gradient at the unexposed face remains the same (i.e. zero). The dimensionless form of eq. (20) can be solved using these conditions to obtain the moisture distribution during the falling-rate period in dimensionless form as (Puyate, 1999)

$$\theta_2(Y,s) = \frac{4}{\pi}\sum_{k=1}^{\infty} H_k \exp[-(2k-1)^2\pi^2 s/4]\cos[(2k-1)\pi Y/2] \tag{24}$$

where $s = \tau - \tau_{cr}$ and

$$H_k = \frac{(-1)^k}{(2k-1)}\left\{\mu\left[\tau_{cr} + \frac{1}{3} - \frac{4}{\pi^2(2k-1)^2} - \frac{2(2k-1)^2}{\pi^2}\sum_{n=1}^{\infty}\frac{\exp(-n^2\pi^2\tau_{cr})}{n^2[(2k-1)^2 - 4n^2]}\right] - 1\right\} \tag{25}$$

The total quantity of moisture in the body at any time during the falling-rate period is obtained by integrating eq. (24) across the thickness as

$$\Theta_2(s) = -\frac{8}{\pi^2}\sum_{k=1}^{\infty}\frac{(-1)^k}{(2k-1)} H_k \exp[-(2k-1)^2\pi^2 s/4] \tag{26}$$

In contrast to the above, Sherwood (1931) analysed an infinite slab for two cases which may be interpreted in terms of the drying intensity μ as:

(i) $\mu >> 1$; that is, the drying rate is very fast, the constant-rate period is negligible, and the moisture distribution at the beginning of the falling-rate period is approximately the initial uniform moisture concentration. This *Sherwood's high drying rate (HDR) model* for the falling-rate period is given in dimensionless form as

$$\Theta_2(\tau) = \frac{8}{\pi^2}\sum_{k=1}^{\infty}(2k-1)^{-2}\exp[-(2k-1)^2\pi^2\tau/4] \tag{27}$$

(ii) $\mu << 1$; that is, the drying rate is very slow and a parabolic moisture distribution is assumed to exist at the start of the falling-rate period. This *Sherwood's low drying rate (LDR) model* for the falling-rate period is given in dimensionless form as

$$\Theta_2(s) = \frac{32\mu}{\pi^4}\sum_{k=1}^{\infty}(2k-1)^{-4}\exp[-(2k-1)^2\pi^2 s/4] \qquad (28)$$

Figure 2 shows comparison of the drying rate profiles of Sherwood's LDR and HDR models, the exact solution (26), and experimental data on hemlock wood (Puyate, 1999) for $\mu = 2.94$, using eq. (23) for the constant-rate period. Details of this comparison are provided in Puyate (1999). It may be seen that the exact solution (26) compares well with the experimental data, but the LDR solution under-predicts the critical time and the drying rate in the early stages of the falling-rate period. For short times or high moisture content, the HDR solution over-predicts the drying rate in the constant-rate period. For longer times or small moisture content, the HDR solution under-predicts the drying rate. For this value of μ, the errors in the two approximate solutions are of similar magnitude. The main difference between Sherwood's solutions and the exact solution is in the length of the constant-rate period which results in the under-prediction of the drying time in the falling-rate period.

DISCUSSION AND CONCLUSION

The theory is presented for the drying characteristics of an elastic flat plate with a receding evaporative front. A three-stage drying process is proposed in which the first stage is saturated. During the second stage (partially saturated stage), the receding evaporative front divides the material into two regions; an unsaturated region between the surface of the drying material and the evaporative front, and a saturated region between the evaporative front and the unexposed face of a material with a fixed base. In the third stage (fully unsaturated stage), the saturated region of the partially saturated stage is obliterated and the body is entirely unsaturated. Fluid flow in the saturated part of the body is governed by capillary pressure according to Darcy's Law. Moisture transport in the unsaturated part of the body may be described by Sherwood's diffusion theory, upon which an exact model is presented here for the falling-rate period. The exact model captures the true moisture distribution at the end of the constant-rate period, while Sherwood's models are based on assumed uniform and parabolic moisture distributions at the end of the constant-rate period. For $\mu = 2.94$, the moisture distribution at the end of the constant-rate period is neither uniform nor parabolic (Puyate, 1999), and this explain the deviation of Sherwood's models from the exact model and the experimental data in Fig. 2. Sherwood's models, however, compare reasonably well with the exact model and with experimental data at values of μ corresponding to the assumed initial conditions of these models (Puyate, 1999). On the whole, the proposed three-stage drying process may be characterized by coupling Scherer's model and Sherwood's model in a unified treatment as discussed in Parts II and III of this series.

ACKNOWLEDGEMENT

I would like to thank C. J. Lawrence for his contribution to this paper.

REFERENCES

Aris, R., 1962, Vectors, Tensors, and the Basic equations of Fluid mechanics, Dover Publications, New -York.

Brinker, C. J., and Scherer, G. W., 1990, *Sol-Gel Science*, Academic Press, New York.

Ford, R. W., 1986, Ceramics Drying, Pergamon Press, Oxford.

Gilliland, E. R., and Sherwood, T. K., 1933,. The drying of solids VI, Industrial and Engineering Chemistry, 25: 1134-1136.

Keey, R. B., 1975. Drying Principles and Practice, 2nd ed., Pergamon Press, Oxford.

Landau, L. D., and Lifshitz, E. M., 1986, Theory of Elasticity, 3rd ed., Pergamon Press, Oxford.

Puyate, Y. T., 1999. Diffusion in Fine Tubes and Pores, Ph.D. Thesis, University of London

Scherer, G. W., 1987a. Drying gels II: Film and flat plate, Journal of Non-Crystalline Solids, 89: 217-238.

Scherer, G. W., 1987b. Drying gels V: Rigid gels, Journal of Non-Crystalline Solids, 92: 122-124.

Scherer, G. W., 1990,. Theory of drying, Journal of the American Ceramic Society, 73: 3-14.

Sherwood, T. K., 1929. The drying of solids I, Industrial and Engineering Chemistry, 21: 12-14.

Sherwood, T. K., 1931. Application of theoretical diffusion equations to the drying of solids, *Trans. AIChE*, 27, pp. 190-200.

Terzaghi, K., Peck, R. B., and Mesri, G., 1996. Soil Mechanics in Engineering Practice, 3rd ed., Wiley, New York.